Journal of Asian Ceramic Societies 2 (2014) 20–26

Contents lists available at ScienceDirect

Journal of Asian Ceramic Societies

journal homepage: www.elsevier.com/locate/jascer

Synthesis and electrical properties of $(1-x)(Na_{0.5}Bi_{0.5})TiO_3-xBa(Mg_{0.5}W_{0.5})O_3$ piezoelectric ceramics

Takeshi Kimura[a,*], Shu Yin[a], Qiang Dong[a], Xiaoyong Wu[a], Ryusuke Akita[a], Takatoshi Hashimoto[b], Atsushi Sasaki[b], Shuji Aisawa[b], Tsugio Sato[a]

[a] Institute of Multidisciplinary Research for Advanced Materials, Tohoku University, 2-1-1, Katahira, Aoba-ku, Sendai 980-8577, Japan
[b] NEC Tokin Corporation, 6-7-1 Koriyama, Taihaku-ku, Sendai 980-8510, Japan

ARTICLE INFO

Article history:
Received 11 October 2013
Received in revised form 2 December 2013
Accepted 9 December 2013
Available online 31 December 2013

Keywords:
$Na_{0.5}Bi_{0.5}TiO_3$
Solvothermal approach
Orientation
Piezoelectricity
Morphotropic phase boundary (MPB)

ABSTRACT

$(1-x)(Na_{0.5}Bi_{0.5})TiO_3-xBa(Mg_{0.5}W_{0.5})O_3$ particles with $x = 0.00–0.08$ were synthesized by a solvothermal approach at 230 °C for 48 h. The results of X-ray diffraction analysis revealed a rhombohedral–tetragonal morphotropic phase boundary (MPB) composition existed in the range of $x = 0.05–0.06$ at room temperature. The ceramics around the phase boundary composition provide excellent piezoelectric properties, i.e., the highest piezoelectric constant, d_{33}, (108 pC/N) could be realized at x value of 0.05. By using a casting sintering method, the ceramics consisted of the oriented rod-like particles with condensed sintering body were obtained, and the piezoelectric properties could be improved to show such a high piezoelectric constant as $d_{33} = 112$ pC/N at x value of 0.05.

1. Introduction

Lead-based perovskite solid solutions of $Pb(Zr,Ti)O_3$ (PZT) have been widely used for piezoelectric devices due to their large piezoelectric constants at the relatively high temperatures [1,2]. Nowadays, because of the toxicity of lead oxide, it is better to use lead-free piezoelectric materials in lieu of PZT for environmental protection; therefore, there is an increasing interest of investigating lead-free piezoelectric materials. Sodium bismuth titanate, $(Na_{0.5}Bi_{0.5})TiO_3$ (NBT), has been regarded as a promising candidate for lead-free piezoelectric ceramics due to its strong ferroelectricity at room temperature [3]. However, NBT suffers from a poling problem because of its high coercive field ($E_c = 73$ kV/cm) and high conductivity, causing a difficulty in obtaining desired piezoelectric properties. To solve this problem, various NBT-based solid solutions have been developed [4–7]. $Ba(Mg_{0.5}W_{0.5})O_3$ ceramics are expected to have high piezoelectric properties due to their high elastic compliance, S_{ij}, which were calculated by first principles calculations [8]. However, it is difficult to synthesize the single-phase $Ba(Mg_{0.5}W_{0.5})O_3$ by solid-state reaction [9]. Recently, considerable research efforts have been devoted to the preparation of materials by various wet chemical methods, including solvothermal process [10], citrate method [11], emulsion method [12], composite-hydroxide-mediated method [13], etc. It was found that hard synthetic phase or morphologies such as plate-like [14] and cube-like shape [15] particles could be synthesized by the wet processes due to the low reaction temperature and dissolution-recrystallization mechanism. One of the approaches to enhance the piezoelectric properties of lead-free ceramics is the control of the microstructure of ceramics by grain orientation. Some approaches such as reactive-templated grain growth method and templated grain growth method have been carried out [16–21].

In the present study, wire- or rod-like particles of $(1-x)(Na_{0.5}Bi_{0.5})TiO_3-xBa(Mg_{0.5}W_{0.5})O_3$ with $x = 0.00–0.08$ were produced by the solvothermal process and sintered by the casting method to form ceramics consisted of oriented grains, and the piezoelectrical properties of the products were examined.

2. Experimental

2.1. Synthesis

$(1-x)(Na_{0.5}Bi_{0.5})TiO_3-xBa(Mg_{0.5}W_{0.5})O_3$ powders with $x = 0–0.08$ were synthesized by a solvothermal approach.

* Corresponding author. Tel.: +81 22 217 5599; fax: +81 22 217 5598.
E-mail address: takeshik@mail.tagen.tohoku.ac.jp (T. Kimura).

Peer review under responsibility of The Ceramic Society of Japan and the Korean Ceramic Society.

Production and hosting by Elsevier

2187-0764 © 2013 The Ceramic Society of Japan and the Korean Ceramic Society. Production and hosting by Elsevier B.V. All rights reserved.
http://dx.doi.org/10.1016/j.jascer.2013.12.001

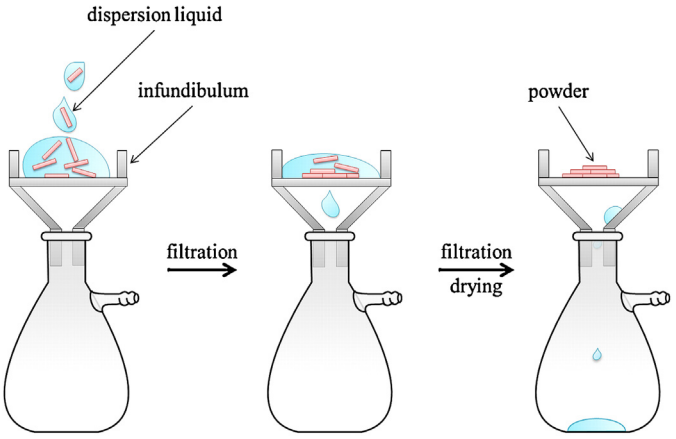

Fig. 1. A casting process with filtration system.

$Ba(OH)_2{\cdot}8H_2O$, $Bi(NO_3)_3{\cdot}5H_2O$, $Na_2WO_4{\cdot}2H_2O$, $Mg(NO_3)_2{\cdot}6H_2O$, $Ti(i\text{-}PrO)_4$ and Li_2CO_3 (sintering additive [22]) were used as starting materials. Firstly, 40 mmol $Ti(i\text{-}PrO)_4$ was dissolved in 15 mL isopropanol, and then desired amount of $Ba(OH)_2{\cdot}8H_2O$, $Bi(NO_3)_3{\cdot}5H_2O$, $Na_2WO_4{\cdot}2H_2O$, $Mg(NO_3)_2{\cdot}6H_2O$, 0.60 mmol Li_2CO_3 and 35 mL NaOH aqueous solutions (12 M) were added to the precipitate amorphous gel. Then, the slurry solution was introduced into a Teflon®-lined stainless autoclave with a 100 cm^3 of internal volume. The autoclave was sealed and heated at 230 °C for 48 h in an electric oven, where the autoclave was rotated at 50 rpm during the reaction using a rotation type hydrothermal reaction apparatus [23]. After that, the autoclave was taken out to allow cooling to room temperature. The resulting white powders were washed with distilled water and ethanol. Finally, they were dried at 60 °C for 1 h, and calcined at 600 °C for 1 h.

2.2. Characterizations

The particle morphology was observed by a scanning electron microscope (SEM. Hitachi S-4800). The X-ray diffraction (XRD) analysis of the obtained powder samples and sintered ceramics was carried out using CuKα radiation with a pyrolytic graphite monochromator mounted powder diffractometer (Bruker, D2 PHASER). The ceramic discs were sintered by a conventional sintering method or the casting method. In a conventional sintering method, the sample powders were uniaxially pressed at 20 MPa in a steel die to form pellets of 20 mm in diameter and 3 mm in thickness, and then isostatically pressed at 200 MPa. On the other hand, in the casting method, the sample powders were dispersed in ethanol, cast on an infundibulum, filtered before uniaxially pressed at 20 MPa (Fig. 1), and then isostatically pressed at 200 MPa. Each pellet was sintered at 1100 °C for 2 h.

The fracture surfaces of the sintered bodies were observed by a scanning electron microscope (SEM. Hitachi S-4800). The densities of the sintered pellets were measured by the Archimedes' method. The lattice parameters were evaluated by X-ray diffraction analysis using the Rietveld refinement with the RIETAN-FP program [24]. Measurements for Rietveld refinements were carried out at 40 kV and 30 mA over the 2θ range of 10–130° with a 0.02° of 2θ step size, and around 0.3 s of count time, to ensure the maximum intensity of XRD patterns reach up to 10,000 counts (Bruker, D2 PHASER).

The upper and bottom surfaces of specimens were coated with gold paste and fired at 800 °C for 20 min before the electrical measurements. Prior to piezoelectric measurements, the sintered bodies were shaped as a disk of size 15ϕ × 1.0 mm for the k_p, ${S_{11}}^E$, ${\varepsilon_{33}}^T/\varepsilon_0$, Q_m and *phase angle* determination, and then the poling

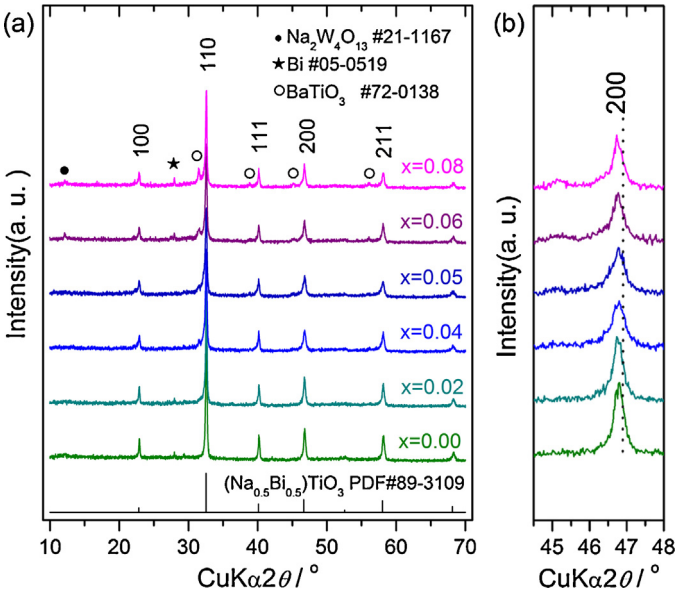

Fig. 2. XRD patterns of $(1-x)(Na_{0.5}Bi_{0.5})TiO_3-xBa(Mg_{0.5}W_{0.5})O_3$ powders (x = 0.00–0.08) formed by the solvothermal reaction at 230 °C for 48 h followed by calcinations at 600 °C for 1 h in the 2θ ranges of (a) 10–70° and (b) 44.5–48°.

treatment was performed in a silicon oil bath at 80 °C by applying a DC electric field of 3.0 kV/mm for 30 min (Withstanding Voltage Tester, TOS 5101). The piezoelectric constant, d_{33}, of the samples was measured by means of a quasi-static d_{33} meter (IACAS, ZJ-3BN) based on the Berlincourt method at 110 Hz. The dielectric properties (ε_r and ${\varepsilon_{33}}^T/\varepsilon_0$) and other piezoelectric properties (k_p, ${S_{11}}^E$, Q_m and *phase angle*) were measured using an Agilent 4294A precision impedance analyzer and calculated according to the IRE standards by the resonant–antiresonant method [25].

3. Results and discussion

Fig. 2 shows the X-ray diffraction patterns of $(1-x)(Na_{0.5}Bi_{0.5})TiO_3-xBa(Mg_{0.5}W_{0.5})O_3$ powders with x = 0–0.08 formed by the solvothermal reaction at 230 °C for 48 h, followed by calcination at 600 °C for 1 h. The samples consisted of the single phase of $(Na_{0.5}Bi_{0.5})TiO_3$ (PDF#01-089-3109) structure with $x < 0.06$. However, the peaks attributed to $BaTiO_3$ phase, $Na_2W_4O_{13}$ phase and Bi phase were observed for the specimens with $x \geq 0.06$. In Fig. 2(b), when the $Ba(Mg_{0.5}W_{0.5})O_3$ content varies from 0.00 to 0.08, the (2 0 0) peak near 47° tends to shift slightly toward lower diffraction angles, as indicated in the enlargement of the peak. This indicates that a very small amount of $Ba(Mg_{0.5}W_{0.5})O_3$ entered in the matrix of the $(Bi_{0.5}Na_{0.5})TiO_3$ according to Bragg's equation ($2d \sin\theta = \lambda$). However, when a large amount of $Ba(Mg_{0.5}W_{0.5})O_3$ was added into the specimen, excess Ba, Mg and W ions reacted with the ions in the matrix to form impurity compounds.

Fig. 3 shows the SEM images of as-prepared powders. The $(1-x)(Na_{0.5}Bi_{0.5})TiO_3-xBa(Mg_{0.5}W_{0.5})O_3$ samples consisted of the rod-like particles with diameters of 50 nm and lengths of up to several tens of micrometers together with micro-cubes of 0.5–4.0 μm of one side length. As shown in Fig. 2, the samples consisted of the single phase of $(Na_{0.5}Bi_{0.5})TiO_3$ structure with $x < 0.06$, indicating that both rod-like and cube-like particles are the same $(Na_{0.5}Bi_{0.5})TiO_3$ compound, although the formation process of them during the solvothermal process might be different.

Fig. 4 shows the X-ray diffraction patterns of undoped $(Na_{0.5}Bi_{0.5})TiO_3$ powders synthesized by the solvothermal reactions at 230 °C for 6 h and 48 h. Although the sample synthesized for

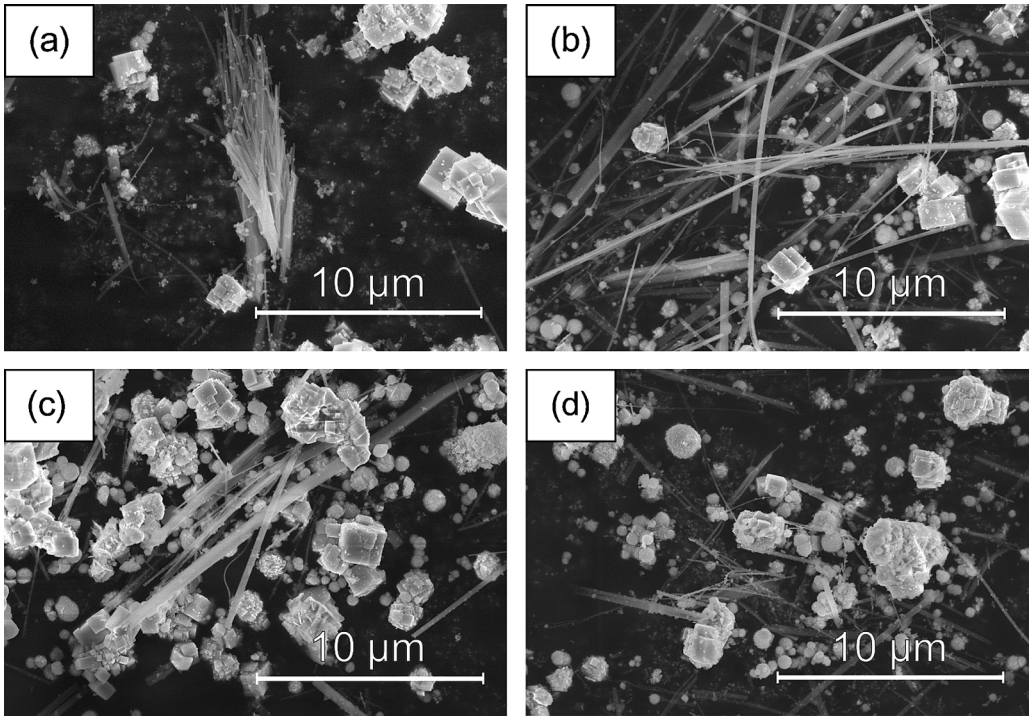

Fig. 3. SEM images of $(1-x)(Na_{0.5}Bi_{0.5})TiO_3-xBa(Mg_{0.5}W_{0.5})O_3$ powders with (a) $x = 0.000$, (b) $x = 0.020$, (c) $x = 0.035$, and (d) $x = 0.050$ formed by the solvothermal reaction at 230 °C for 48 h followed by calcinations at 600 °C for 1 h.

48 h was a single phase of $(Na_{0.5}Bi_{0.5})TiO_3$, the sample synthesized for 6 h showed a second phase of $Bi_4Ti_3O_{12}$ (PDF#01-089-7500) structure. It was reported that the $Bi_4Ti_3O_{12}$ crystal tended to grow as rod-like shape particle [26,27]. In contrast, the $(Na_{0.5}Bi_{0.5})TiO_3$ compound tends to grow as cube-like particles due to the perovskite cubic or rhombohedral structures. Therefore, the rod-like particles of $(1-x)(Na_{0.5}Bi_{0.5})TiO_3-xBa(Mg_{0.5}W_{0.5})O_3$ shown in Fig. 3 might be obtained via the formation of $Bi_4Ti_3O_{12}$ as an intermediate precursor, while the cubic-like ones might be produced via the formation of $(Na_{0.5}Bi_{0.5})TiO_3$ precursor.

The samples were sintered at 1100 °C for 2 h with heating rate of 10 °C/min, by the conventional sintering method and casting sintering method, respectively. Fig. 5 shows the scanning electron micrographs (SEM) of the fracture surfaces of the $(1-x)(Na_{0.5}Bi_{0.5})TiO_3-xBa(Mg_{0.5}W_{0.5})O_3$ ($x = 0$–0.050) ceramics sintered at 1100 °C for 2 h. After sintering, the rod-like morphology was still apparently maintained for $x = 0.00$ composition, indicating that the rod-like grains resulted in an orientation growth by a casting sintering, but in a random growth by a conventional sintering. On the other hand, for $x = 0.035$ and 0.050 compositions, the number of rod-like grains by both sintering method decreased and no obvious differences were observed. In Fig. 5(a) and (b), by the conventional sintering method and the casting sintering method, the average diameter of each undoped $(Na_{0.5}Bi_{0.5})TiO_3$ grain except for rod-like one was almost the same value around 20 μm. The average diameter decreased from 20 μm to several μm with an increase in the amount of $Ba(Mg_{0.5}W_{0.5})O_3$. This result indicated that the grain growth of specimens was greatly depressed by doping small amounts of Ba, Mg and W ions. Similar results were reported by adding excess amounts of Na, Bi and Ti ions in the $(K_{0.5}Na_{0.5})(Nb_{1-x}Ta_x)O_3-K_{5.4}CuTa_{10}O_{29}$ ceramics [28].

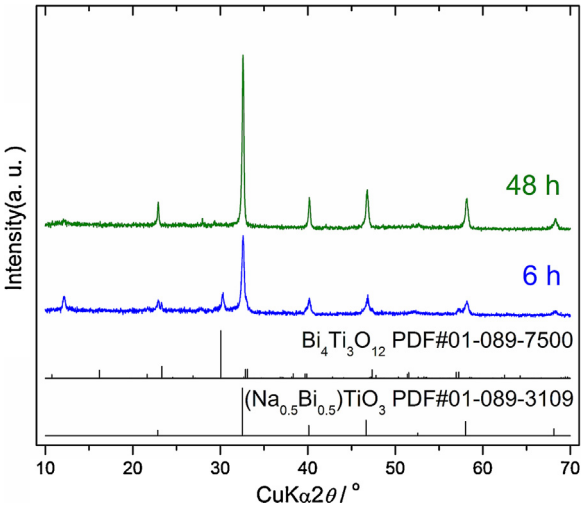

Fig. 4. XRD patterns of the undoped $(Na_{0.5}Bi_{0.5})TiO_3$ powders synthesized by the solvothermal reactions at 230 °C for 6 and 48 h.

Fig. 6 shows the XRD patterns of the $(1-x)(Na_{0.5}Bi_{0.5})TiO_3-xBa(Mg_{0.5}W_{0.5})O_3$ ($x = 0$–0.08) ceramics sintered at 1100 °C for 2 h by the casting sintering method. The ceramics consisted of the single phase of $(Na_{0.5}Bi_{0.5})TiO_3$ (PDF#01-089-3109) structure with $x < 0.06$. However, the peak of Na_3BiO_3 phase was observed for the specimens with $x \geq 0.06$. Although the samples for $x = 0.06$ and 0.08 compositions had impurity phase, the peaks shifted slightly toward the lower diffraction angles with the increment of x values in the sample. The rhombohedral symmetry of pure $(Na_{0.5}Bi_{0.5})TiO_3$ at room temperature is characterized by a (0 0 3)/(0 2 1) peak splitting between 39.0° and 41.5° and a single (2 0 2) peak between 44.5° and 48.0°. In Fig. 6(b), the (0 0 3)/(0 2 1) peak splitting is still distinguishable until $x = 0.06$. In Fig. 6(c), a distinct peak splitting can be seen at $x \geq 0.05$ and beyond, corresponding to a tetragonal symmetry. Therefore, it can be inferred that the MPB of $(1-x)(Na_{0.5}Bi_{0.5})TiO_3-xBa(Mg_{0.5}W_{0.5})O_3$ ceramics lies within the composition range of $0.05 \leq x \leq 0.06$

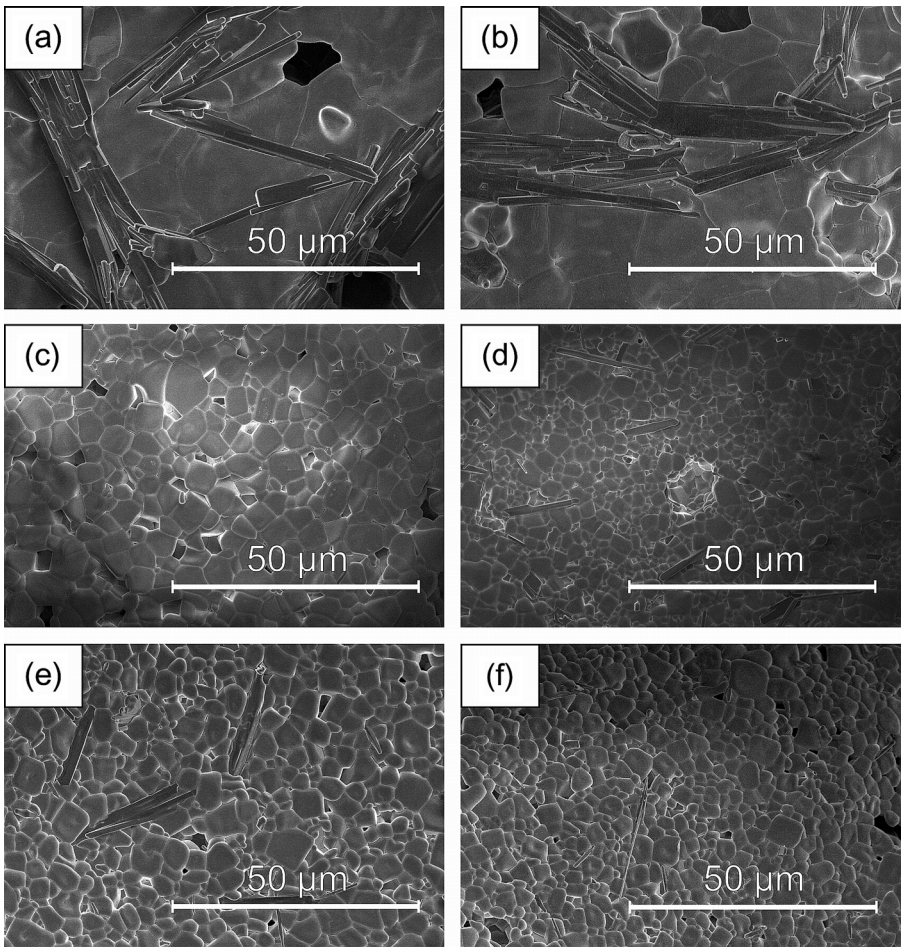

Fig. 5. SEM images of the fracture surfaces of $(1-x)(Na_{0.5}Bi_{0.5})TiO_3-xBa(Mg_{0.5}W_{0.5})O_3$ ceramics ($x = 0.000–0.050$) sintered at 1100 °C for 2 h by (a, c, e) the conventional sintering method and (b, d, f) casting sintering method. The $Ba(Mg_{0.5}W_{0.5})O_3$ molar fraction: (a, b) 0.000, (c, d) 0.035, and (e, f) 0.050.

at room temperature, where the rhombohedral and tetragonal phases coexist.

Fig. 7 shows the lattice parameters and lattice volumes of the sintered bodies by the conventional sintering method and casting sintering method for the rhombohedral ferroelectric phase. The lattice parameters of the samples by the conventional sintering method and casting sintering method showed the similar tendency with the amount of $Ba(Mg_{0.5}W_{0.5})O_3$. The lattice parameter of a monotonously increased with an increase in $Ba(Mg_{0.5}W_{0.5})O_3$ content. On the other hand, the lattice parameter of *c* and lattice

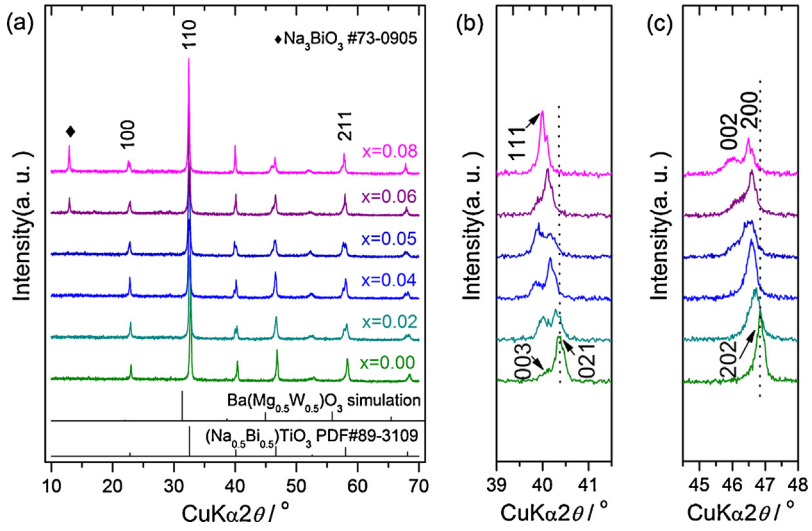

Fig. 6. XRD patterns of $(1-x)(Na_{0.5}Bi_{0.5})TiO_3-xBa(Mg_{0.5}W_{0.5})O_3$ ceramics ($x = 0.00–0.08$) sintered at 1100 °C for 2 h by the casting sintering method in the 2θ ranges of (a) 10–70°, (b) 39.0–41.5°, and (c) 44.5–48.0°.

Table 1
(a) bulk density, ρ, (b) relative density, ρ', (c) electromechanical coupling factor, k_p, (d) piezoelectric constant, d_{33}, (e) elastic compliance, $S_{11}{}^E$, (f) relative dielectric constant, $\varepsilon_{33}{}^T/\varepsilon_0$, (g) mechanical quality factor, Q_m, and (h) *phase angle* of $(1-x)(Na_{0.5}Bi_{0.5})TiO_3-xBa(Mg_{0.5}W_{0.5})O_3$ ceramics (x = 0.00–0.06) sintered at 1100 °C for 2 h by the conventional sintering method.

	No-casting	0.01	0.02	0.035	0.045	0.05	0.055	0.06
a	ρ (g/cm^3)	5.57	5.62	5.56	5.63	5.61	5.66	5.31
b	ρ' (%)	93.1	94.1	92.7	94.1	93.5	94.6	88.9
c	k_p (%)	6.42	8.18	20.4	18.9	24.7	15.6	8.02
d	d_{33} (pC/N)	37	47	92	100	108	93	34
e	$S_{11}{}^E$ (10^{-12} m^2/N)	4.31	4.35	4.89	5.05	5.11	4.81	5.09
f	$\varepsilon_{33}{}^T/\varepsilon_0$	359	371	390	437	553	729	5.03
g	Q_m	190	272	286	134	130	107	20.4
h	*Phase angle* (°)	−52.6	−14.3	68.7	37.5	60.3	22.4	−81.6

Table 2
(a) density, ρ, (b) relative density, ρ', (c) electromechanical coupling factor, k_p, (d) piezoelectric constant, d_{33}, (e) elastic compliance, $S_{11}{}^E$, (f) relative dielectric constant, $\varepsilon_{33}{}^T/\varepsilon_0$, (g) mechanical quality factor, Q_m, and (h) *phase angle* of $(1-x)(Na_{0.5}Bi_{0.5})TiO_3-xBa(Mg_{0.5}W_{0.5})O_3$ ceramics (x = 0.00–0.06) sintered at 1100 °C for 2 h by the casting sintering method.

	Casting	0.01	0.02	0.035	0.045	0.05	0.06
a	ρ (g/cm^3)	5.60	5.65	5.68	5.54	5.71	5.37
b	ρ' (%)	93.7	94.6	94.7	92.6	95.3	92.6
c	k_p (%)	7.93	10.7	21.9	15.4	26.5	7.97
d	d_{33} (pC/N)	54	63	94	94	112	70
e	$S_{11}{}^E$ (10^{-12} m^2/N)	4.27	4.12	4.54	4.31	5.02	3.80
f	$\varepsilon_{33}{}^T/\varepsilon_0$	341	402	429	462	594	2.99
g	Q_m	591	414	277	45.9	166	347
h	*Phase angle* (°)	13.9	34.2	71.4	−35.4	69.0	−10.3

volume increased at first with increasing $Ba(Mg_{0.5}W_{0.5})O_3$ content up to x = 0.05, while the lattice parameter and lattice volume with $x \geq 0.05$ changed irregularly. It might suggest that the rhombohedral phase of $(1-x)(Na_{0.5}Bi_{0.5})TiO_3-xBa(Mg_{0.5}W_{0.5})O_3$ crystal changed to tetragonal phase at x value of around 0.05.

Tables 1 and 2 and Fig. 8 summarize the bulk density (ρ), relative density (ρ'), electromechanical coupling factor (k_p), piezoelectric constant (d_{33}), elastic compliance ($S_{11}{}^E$), relative dielectric constant ($\varepsilon_{33}{}^T/\varepsilon_0$), mechanical quality factor (Q_m), and *phase angle* of $(1-x)(Na_{0.5}Bi_{0.5})TiO_3-xBa(Mg_{0.5}W_{0.5})O_3$ ceramics (x = 0.00–0.06) sintered at 1100 °C for 2 h by the conventional sintering method and casting sintering method. With increasing the molar fraction of $Ba(Mg_{0.5}W_{0.5})O_3$, the k_p, d_{33}, $S_{11}{}^E$, and *phase angle* firstly increased, reached to a maximum value and then decreased. Generally, the ceramics around the phase boundary composition provide excellent piezoelectric properties. The highest values of k_p, d_{33}, $S_{11}{}^E$, and *phase angle* for $(1-x)(Na_{0.5}Bi_{0.5})TiO_3-xBa(Mg_{0.5}W_{0.5})O_3$ with x = 0.05 by the conventional sintering method were 24.7%, 108 pC/N, 5.11×10^{-12} m^2/N, and 60.3°, respectively. These piezoelectric properties demonstrate that the compositions near the MPB have relatively high piezoelectric and electromechanical activities due to the increment of the number of possible spontaneous polarization and also the coexistence of rhombohedral and tetragonal phases. The increase in the value of the *phase angle* by doping with $Ba(Mg_{0.5}W_{0.5})O_3$ might contribute to decrease the coercive field (E_c). By using the casting sintering method, the densities of ceramics are higher than that by the conventional sintering method, the rod-like particles were orientated in the sintered body, and the piezoelectric properties were improved, i.e., the highest values of k_p, d_{33}, $S_{11}{}^E$, and *phase angle* for $(1-x)(Na_{0.5}Bi_{0.5})TiO_3-xBa(Mg_{0.5}W_{0.5})O_3$ with x = 0.05 by the casting sintering method were 26.5%, 112 pC/N, 5.02×10^{-12} m^2/N, and 69.0°, respectively. Furthermore, when the casting sintering method is compared with the conventional method, the differences of d_{33} were large for $x \leq 0.0.2$, while small for $0.035 \leq x \leq 0.05$. In Fig. 5, the orientation growth of rod-like grains can be apparently observed for x = 0.00 composition, but there were few rod-like grains for x = 0.035 and 0.050 compositions. Therefore, the piezoelectric properties were improved due to increase in the density of the sample by casting sintering, and the improvement of the piezoelectric constant might be related to the orientation of rod-like particles.

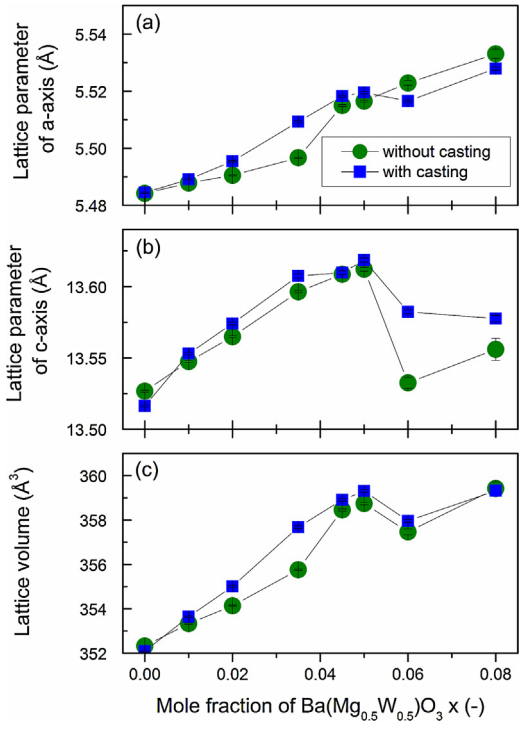

Fig. 7. (a) and (b) lattice parameters and (c) lattice volume of $(1-x)(Na_{0.5}Bi_{0.5})TiO_3-xBa(Mg_{0.5}W_{0.5})O_3$ ceramics (x = 0.00–0.08) sintered at 1100 °C for 2 h by the conventional sintering method and casting sintering method.

It was reported that the piezoelectric constant, electromechanical coupling factor and depolarization temperature of $(1-x)(Na_{0.5}Bi_{0.5})TiO_3-xBaTiO_3$ ceramics made by the citrate

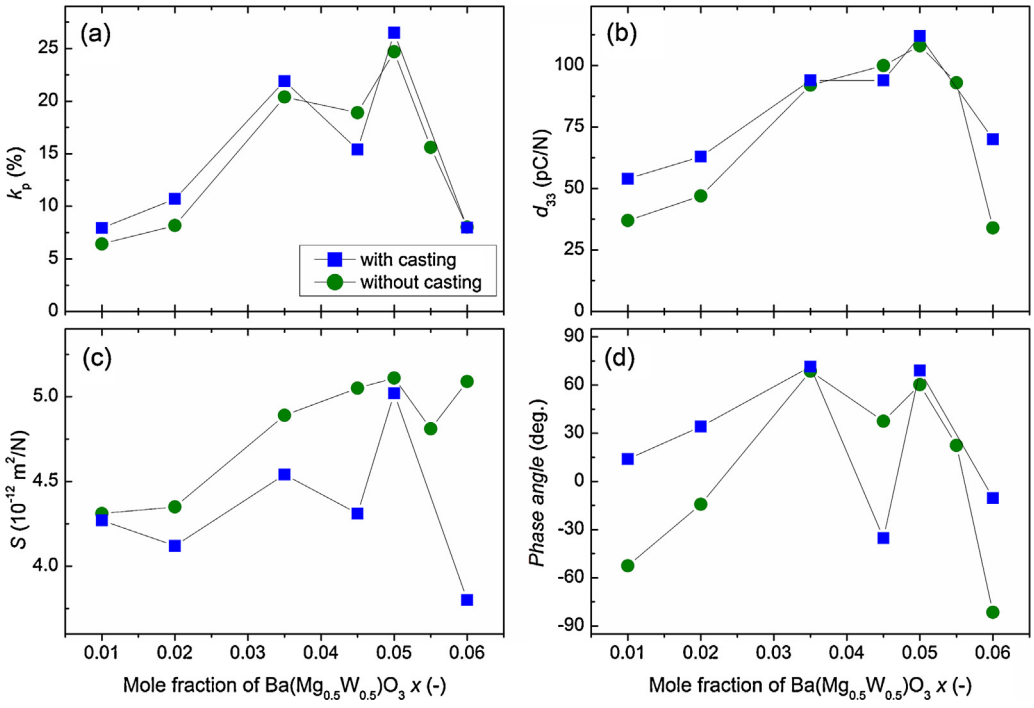

Fig. 8. The values of (a) electromechanical coupling factor, k_p, (b) piezoelectric constant, d_{33}, (c) elastic compliance, $S_{11}{}^E$, and (d) *phase angle* of $(1-x)(Na_{0.5}Bi_{0.5})TiO_3-xBa(Mg_{0.5}W_{0.5})O_3$ ceramics (x = 0.00–0.06) sintered at 1100 °C for 2 h by the conventional sintering method and the casting sintering method as a function of $Ba(Mg_{0.5}W_{0.5})O_3$ concentration.

method reached to the maximum values of d_{33} = 176 pC/N, k_p = 21.2% and T_d = 88 °C at x = 0.06 [29], which agreed with the high electromechanical coupling factor and depolarization temperature (in Fig. 9) in the present research.

Fig. 9 shows the temperature dependence of the dielectric constant (ε_r) and dielectric loss ($\tan\delta$) for unpoled $(1-x)(Na_{0.5}Bi_{0.5})TiO_3-xBa(Mg_{0.5}W_{0.5})O_3$ ceramics at frequencies ranging from 1 to 100 kHz. For the specimen with the composition of x = 0.00, two abnormal dielectric peaks were observed during the heating process. On the other hand, for other specimens ($x \geq 0.030$), one abnormal dielectric peak was observed. The temperature corresponding to the peak in the low

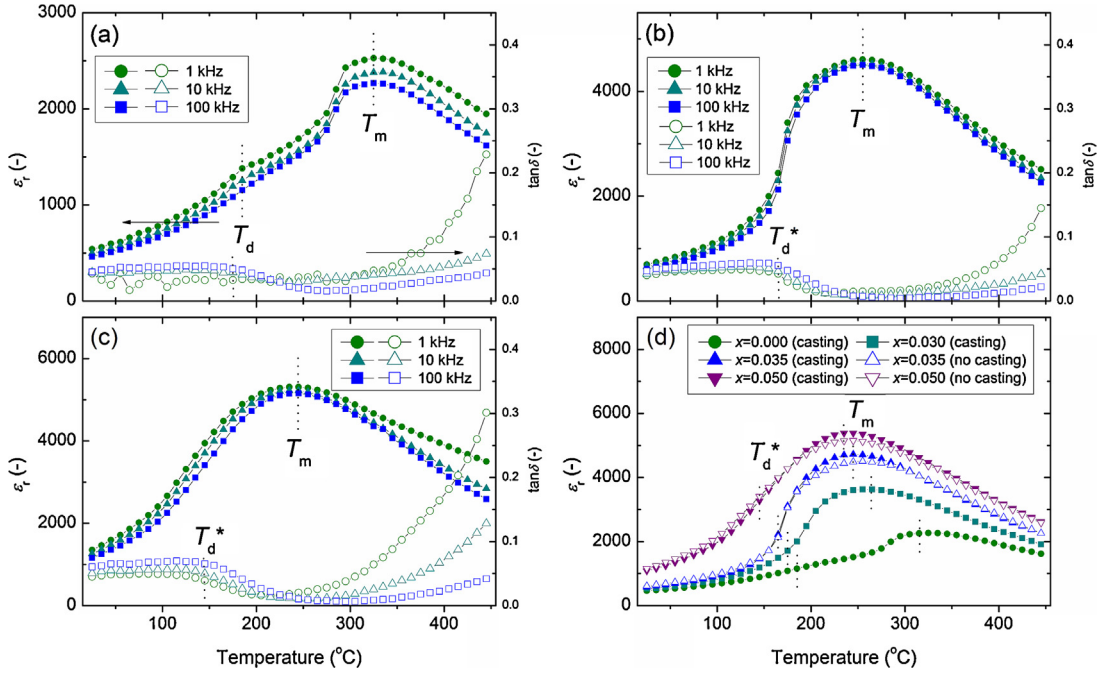

Fig. 9. Temperature dependence of the dielectric constant of $(1-x)(Na_{0.5}Bi_{0.5})TiO_3-xBa(Mg_{0.5}W_{0.5})O_3$ ceramics at frequencies ranging from 1 to 100 kHz with (a) x = 0, (b) x = 0.035, and (c) x = 0.050 sintered at 1100 °C for 2 h by the casting sintering method, and (d) frequencies ranging at 100 kHz with x = 0–0.050 sintered at 1100 °C for 2 h by the conventional sintering method and casting sintering method.

temperature range is denoted as depolarization temperature (T_d), and the temperature corresponding to the maximum value of dielectric constant is referred to as the maximum temperature (T_m). For $x \geq 0.03$ compositions, the peaks showing depolarization temperature of specimens could not be found by the dielectric constant data. Following Hiruma et al., the depolarization temperature T_d* could be defined as the first peak in the dielectric loss curve of the poled samples as a function of temperature [30,31]. However, the T_d* values determined using two tangent lines on the dielectric loss-temperature curves for the unpoled samples were lower than that for poled samples or that determined using pyroelectric measurements [31,32]. Depolarization in the vicinity of T_d arises from an electric field induced ferroelectric to intermediate antiferroelectric state [33–35]. The MPB compositions exhibit a lower depolarization temperature, suggesting the strong composition-dependent behavior. Very similar behavior has recently been reported in closely related to doped (Na, Bi)TiO_3 systems by Bai et al. [36].

4. Conclusion

The piezoelectric properties of $(Na_{0.5}Bi_{0.5})TiO_3$ were successfully improved by doping with $Ba(Mg_{0.5}W_{0.5})O_3$ and using the cast sintering. The powders synthesized by the solvothermal approach consisted of rod-like particles. The resulting $(1-x)(Na_{0.5}Bi_{0.5})TiO_3-xBa(Mg_{0.5}W_{0.5})O_3$ ceramics exhibit excellent piezoelectric properties around the rhombohedral–tetragonal morphotropic phase boundary. The piezoelectric constant attains a maximum value of $d_{33} = 108$ pC/N at $x = 0.05$. By using the casting sintering method, the sintering property was improved and the rod-like particles were orientated in the ceramics, and the d_{33} of the $(1-x)(Na_{0.5}Bi_{0.5})TiO_3-xBa(Mg_{0.5}W_{0.5})O_3$ with $x = 0.05$ was improved to such a high value as 112 pC/N.

Acknowledgment

This research was partly supported by Scientific Measurements Research Foundation.

References

[1] G.H. Haertling, J. Am. Ceram. Soc., 82, 797–818 (1999).
[2] L.H. Luo, H. Zhu, C.S. Zhao, H.X. Wang and H.S. Luo, Appl. Phys. Lett., 90, 052904–052910 (2007).
[3] A.G. Smolenskii, V. Isupov, I.A. Agranovskaya and N.N. Krainik, Sov. Phys. Solid state (Engl. Transl.), 2, 2651–2654 (1961).
[4] T. Takenaka, K. Maruyama and K. Sakata, Jpn. J. Appl. Phys., 30, (9B) 239–2236 (1991).
[5] N. Ichinose and K. Udagawa, Ferroelectrics, 169, 317–332 (1995).
[6] T. Okuda and K. Takegahara, Ferroelectrics, 196, 175–178 (1997).
[7] T. Takenaka, Ferroelectrics, 230, 87–98 (1999).
[8] Y. Kitanaka, Y. Noguchi and M. Miyayama, Key Eng. Mater., 445, 59–62 (2010).
[9] H.P. Jason, H. Ashfia and L. Hans-Conradzur, J. Solid State Chem., 184, 2293–2298 (2011).
[10] J. Magder, S.M. Vukasovich and J.R. Lockhart, J. Am. Ceram. Soc., 49, 291–295 (1966).
[11] S. Chen, W. Chen, D. Huang, J. Zhou, H. Sun and Y. Li, J. Mater. Sci., 41, 6146–6149 (2006).
[12] Y. Yamashita and H. Yamamoto, J. Eur. Ceram. Soc., 25, 2739–2742 (2005).
[13] S. Yin, T. Hashimoto, Y. Tokano, A. Sasaki and T. Sato, J. Eur. Ceram. Soc., 30, 699–704 (2010).
[14] S.T. McKinstry and G.L. Messing, J. Am. Ceram. Soc., 83, 113–118 (2000).
[15] Y. Hou, B. Liu and L. Wei, Ceram. Int., 35, 1423–1427 (2009).
[16] A.D. Payne, J. Am. Ceram. Soc., 86, (5) 769–774 (2003).
[17] Y. Saito, Y. Aoki and K. Horibuchi, Key Eng. Mater., 320, 3–6 (2006).
[18] T. Toshihiko and S. Yasuyoshi, Jpn. J. Appl. Phys., 38, 5553–5556 (1999).
[19] T. Toshihiko and S. Yasuyoshi, Jpn. J. Appl. Phys., 39, 5577–5580 (2000).
[20] R. Hong, J. Liu, Y. Yao and C. Tian, J. Eur. Ceram. Soc., 28, 2063–2070 (2008).
[21] K. Takeda, T. Muraishi, H. Kakemoto, T. Tsurumi and T. Kimura, Jpn. J. Appl. Phys., 46, 7039–7043 (2007).
[22] Q. Dong, S. Yin, T. Hashimoto, A. Sasaki and T. Sato, J. Eur. Ceram. Soc., 33, 1009–1015 (2013).
[23] S. Yin, T. Takatoshi, Y. Tokano, A. Sasaki and T. Sato, Mater. Res. Bull., 45, 1345–1350 (2010).
[24] T. Ikeda, Matter. Sci. Forum, 321, 198–205 (2000).
[25] Proc. IRE, 49, 1161–1169 (1961).
[26] J. Wang, J. Electroceram., 16, 477–481 (2006).
[27] Z. Ruzhong and L. Danya, J. Alloy. Compd., 519, 25–28 (2012).
[28] K. Kikuta and S. Hirano, J. Appl. Phys., 97, 114105 (2005).
[29] Q. Xu, B.H. Kim, B.K. Ahn, J.H. Ko, W.J. Kang and O.J. Nam, J. Eur. Ceram., 28, 843–849 (2008).
[30] H. Nagata and T. Takenaka, J. Appl. Phys., 104, 124106 (2008).
[31] H. Nagata and T. Takenaka, Jpn. J. Appl. Phys., 45, 7409–7412 (2006).
[32] A.B. Kounga, E. Aulbach, W. Jo, T. Granzow, H. Ehrenberg and J. Rodel, J. Appl. Phys., 103, 034108 (2008).
[33] D. Lin and K.W. Kwok, Solid State Sci., 10, 934–940 (2008).
[34] Y. Masuda, Ferroelectrics, 7, 347–349 (1974).
[35] S.J. Zhang, J. Electroceram., 19, 111–112 (2007).
[36] Y. Bian, J. Hao, B. Shen and J. Zhai, J. Am. Ceram. Soc., 96, 246–252 (2013).